On the Modelling of Carbon Nano Tubes as Generalized Continua

Hossein Aminpour and Nicola Rizzi

Abstract A 1D continuum endowed with internal structure, previously introduced by the authors in order to describe some nonlinear behaviours of Carbon Nano Tubes (CNTs), is extended and generalised by giving a procedure for constructing the constitutive functions. Starting from the reference configuration of a Carbon Nano Sheet (CNS), a Representative Elementary Volume (REV) is chosen. The deformation measures of the REV are identified with the change of the length of the Carbon-Carbon (C-C) bonds and the angle variation between each pair of adjacent bonds. The strain energy density of the REV is given as a standard function of the microscopic strain measures. A relationship between the micro and the continuum strain measures is then put down, this leading to an expression of the strain energy density of the REV in terms of the latter strains. Making the derivative of this energy with respect to its argument the constitutive functions for the 1D continuum are obtained. The geometric and mechanical properties of a graphene nano sheet are used to construct its equivalent continuum and some numerical comparisons are discussed. Although the procedure is set up for a CNS, its extension to Carbon Nano Tubes (CNTs) involves only simple geometric computations.

Keywords Nonlinear elasticity · Bifurcation analysis · Generalized continua · Carbon nano sheets

1 Introduction

CNTs have been given a large attention due to the fact that they show very peculiar mechanical properties (Shima and Sato 2013). In addition, as they can undergo very large deformations without losing the elastic behaviour, nonlinear models must be

H. Aminpour · N. Rizzi (✉)
Università Degli Studi Roma Tre, Via Della Madonna Dei Monti 40, 00184 Roma, Italy
e-mail: nicolaluigi.rizzi@uniroma3.it

H. Aminpour
e-mail: hossein.aminpour@uniroma3.it

H. Altenbach and S. Forest (eds.), *Generalized Continua as Models for Classical and Advanced Materials*, Advanced Structured Materials 42,
DOI 10.1007/978-3-319-31721-2_2

constructed in order to have a fair description of a number of very relevant phenomena. Even though the molecular dynamic approach has been and is still largely used as a simulation tool, it has been recognized as cumbersome in many circumstances. For this reason, the attention of many researchers has been focused on the continuum modelling making recourse to both 3D and shell theories.

Following this line the authors (Aminpour et al. 2014; Aminpour and Rizzi 2015), in accordance with the approach in Antman (2005) and Podio-Guidugli (1982), proposed to use a 1D continuum endowed with a suitable microstructure for the modelling of the mechanical behaviour of CNTs. With respect to a Cosserat beam (Pietraszkiewicz et al. 2007; Bîrsan et al. 2012; Altenbach et al. 2012), that model has one more scalar field which is introduced with the aim of accounting for the deformation of the cross-sections in their own plane. It has been shown that by adopting very simple constitutive relationships—that were polynomial functions up to grade two in the components of the deformation measures—the model is able to capture the relevant phenomena of necking and kinking that appear when a CNT is loaded by two axial forces or two bending moments, at its ends (see Shima and Sato 2013).

The aim of this work is to extend the theory in Aminpour et al. (2014); Aminpour and Rizzi (2015) by proposing a procedure that leads to identify the constitutive relationships of an *equivalent* 1D continuum, starting from the analysis of the microscopic behaviour of a carbon nanomaterial (see e.g. dell'Isola et al. 2012). In view of the results obtained previously, these relationships are given an approximate polynomial expansion of grade two. The analysis is performed for a CNS and, even though it is not presented here, its generalization to CNTs is only matter of simple geometry.

Given a reference configuration of the sheet, a REV including two atoms connected with five C-C bonds connecting themselves and their first neighbours, is considered. By assuming a generic displacement of the six atoms, the change of the lengths of the C-C bonds, together with the angle variation between the adjacent bonds, are assumed as deformation measures of the microscopic model. The strain energy density of the REV is then given in terms of those deformation measures. By assuming a suitable map between the kinematic of the microscopic model and that of the 1D model, the deformation measures of the former are given as functions of the deformation measures of the latter. This allows to write the strain energy density of the REV as a function of the deformation measures of the 1D model. This energy is then assumed as the strain energy density of the 1D continuum *equivalent* to the CNS. Successively, this energy is given a power expansion with respect to the deformation measures, up to the third order. The derivative of the strain energy density with respect to its arguments gives the constitutive relationships of the 1D stress measures.

As a numerical example, the analysis of the mechanical behaviour of a graphene sheet studied in Pei et al. (2010) is performed by means of the geometric model introduced here for two cases of atoms arrangements, namely the so called armchair and zigzag. A trivial nonlinear equilibrium solution is found and the Young's modulus tangent in the origin determined for both the atoms arrangement. The results are found to be in agreement with the values reported in the literature (Xiao et al. 2005;

Lee et al. 2008; WenXing et al. 2004). In addition, a bifurcation analysis has been performed and the bifurcation point on the trivial equilibrium paths for both the armchair and zigzag cases, determined. It is shown that the branched solutions describe a necking phenomenon. Finally we want to stress that only interactions between each atom and its first neighbours have been considered and that to account also for long range interactions would lead to a strain energy density for the equivalent continuum containing gradients of the deformation measures (Alibert et al. 2003).

2 One-Dimensional Beam Model

A beam is thought as a one dimensional continuous body, whose kinematics is described through the placement of the points of a line that we call the beam axis, and the placement of a couple of orthogonal vectors attached to each point of it. They are allowed to change their length in order to describe the cross section deformation. We will consider here a reference configuration φ_0 in which the axis is straight and the sections are orthogonal to it. The axis is described by the function

$$\boldsymbol{q}(s) \qquad s \in [0, 1], \tag{1}$$

where s is its arc length parameter. The unit vector field tangent to the axis of the beam is

$$\boldsymbol{q}'(s), \tag{2}$$

where the prime denotes differentiation with respect to s. Let φ_t be the configuration assumed by the beam during a motion at time t. Such a configuration is described by

- the function $\boldsymbol{p}(s, t)$, providing the present position of $\boldsymbol{q}(s)$;
- a proper orthogonal tensor field $\boldsymbol{R}(s, t)$, providing the rotation of the cross-sections when passing from φ_0 to φ_t ;
- a scalar field $\delta(s, t)$, providing a coarse description of the cross-sections deformation superimposed to the rotation $\boldsymbol{R}(s, t)$.

The tangent vector to the axis of the beam in the present configuration is given by

$$\boldsymbol{p}'(s, t), \tag{3}$$

and the velocity fields are

$$\boldsymbol{w} = \dot{\boldsymbol{p}}, \quad \boldsymbol{W} = \dot{\boldsymbol{R}}\boldsymbol{R}^{\mathrm{T}}, \quad \omega = \dot{\delta}, \tag{4}$$

where $\boldsymbol{W}$ is a skew tensor and the dot denotes differentiation with respect to t. A change of placement is rigid when

$$\boldsymbol{R}' = \boldsymbol{0}, \quad \boldsymbol{p}' = \boldsymbol{R}\boldsymbol{q}', \quad \delta = 0, \tag{5}$$

so that in a rigid motion

$$\dot{\boldsymbol{p}}' = \dot{\boldsymbol{R}}\boldsymbol{q}', \quad \dot{\delta} = 0, \quad \forall t \tag{6}$$

2.1 Strain Measures

Deformation is defined as the difference between the given transplacement and a rigid one. A suitable choice of strain measures with respect to φ_0 is

$$\boldsymbol{e} = \boldsymbol{R}^{\mathrm{T}}\boldsymbol{p}' - \boldsymbol{q}', \quad \boldsymbol{E} = \boldsymbol{R}^{\mathrm{T}}\boldsymbol{R}', \quad \delta, \quad \delta', \tag{7}$$

where $\boldsymbol{E}$ is a skew tensor.

We limit ourselves to the case of a beam whose motion can be described in a 2D subspace of a 3D Euclidean space. Given a fixed orthonormal basis

$$\boldsymbol{D}_1, \boldsymbol{D}_2, \boldsymbol{D}_3 = \boldsymbol{D}_1 \times \boldsymbol{D}_2$$

we assume that $\boldsymbol{q}'(s) = \boldsymbol{D}_1$ so that

$$\boldsymbol{e} = \varepsilon \boldsymbol{D}_1 + \gamma \boldsymbol{D}_2, \quad \boldsymbol{E} = \kappa \boldsymbol{D}_2 \wedge \boldsymbol{D}_1, \tag{8}$$

where ε is the axial strain and γ is the shearing strain, κ denotes the bending curvature.

It is useful to write the strain measures in terms of the displacement field $\boldsymbol{u}$ defined as

$$\boldsymbol{u} = \boldsymbol{p} - \boldsymbol{q} = u\boldsymbol{D}_1 + v\boldsymbol{D}_2 \tag{9}$$

Thus, in view of the definitions (8), (9), the components of the deformation measures (7), read

$$\begin{aligned} \varepsilon &= (1 + u')\cos\vartheta + v'\sin\vartheta - 1, \\ \gamma &= v'\cos\vartheta - (1 + u')\sin\vartheta, \\ \kappa &= \vartheta', \\ \delta, &\quad \delta', \end{aligned} \tag{10}$$

where ϑ is the angle of rotation about $\boldsymbol{D}_3$.

2.2 Balance

The interaction of the beam with the surrounding environment is defined as a linear functional of the velocities (6) and of their first-order derivatives with respect to s, and the external power can be expressed as

$$P_e = \int_0^l (\boldsymbol{b} \cdot \boldsymbol{w} + \boldsymbol{B} \cdot \boldsymbol{W} + \beta \dot{\delta}) \mathrm{d}s + \left[\boldsymbol{t} \cdot \boldsymbol{w} + \boldsymbol{T} \cdot \boldsymbol{W} + \Omega \dot{\delta} \right]_0^l \tag{11}$$

$\boldsymbol{b}$, $\boldsymbol{B}$, β and $\boldsymbol{t}$, $\boldsymbol{T}$, Ω being bulk and contact actions, respectively.

The power expended by the contact actions is a linear functional of the velocity fields and of their first derivatives with respect to X_1, that is

$$P_i = \int_0^l (\boldsymbol{c}_0 \cdot \boldsymbol{w} + \boldsymbol{C}_0 \cdot \boldsymbol{W} + \Delta \dot{\delta} + \boldsymbol{c}_1 \cdot \boldsymbol{w}' + \boldsymbol{C}_1 \cdot \boldsymbol{W}' + \vartheta \dot{\delta}') \mathrm{d}s \tag{12}$$

Following Germain (1973a, b); di Carlo (1996), we require that $P_i = 0$ for any rigid motion, that is true if and only if

$$P_i = \int_0^l (\boldsymbol{c}_1 \cdot \boldsymbol{w}' - (\boldsymbol{p}' \wedge \boldsymbol{c}_1) \cdot \boldsymbol{W} + \boldsymbol{C}_1 \cdot \boldsymbol{W}' + \Delta \dot{\delta} + \vartheta \dot{\delta}') \mathrm{d}s \tag{13}$$

Besides, by requiring that

$$P_e = P_i \qquad \forall t \tag{14}$$

the expressions (11), (13) and (14) give $\boldsymbol{c}_1 = \boldsymbol{t}$, $\boldsymbol{C}_1 = \boldsymbol{T}$ and $\vartheta = \Omega$ and

$$\begin{aligned} \boldsymbol{t}' + \boldsymbol{b} &= \boldsymbol{0}, \\ \boldsymbol{T}' + \boldsymbol{p}' \wedge \boldsymbol{t} + \boldsymbol{B} &= \boldsymbol{0}, \\ \Omega' - \Delta + \beta &= 0 \end{aligned} \tag{15}$$

Equation (15) can be conveniently rewritten in the form

$$\begin{aligned} \boldsymbol{s}' + \boldsymbol{E}\boldsymbol{s} + \boldsymbol{a} &= \boldsymbol{0}, \\ \boldsymbol{S}' + \boldsymbol{E}\boldsymbol{S} - \boldsymbol{S}\boldsymbol{E} + (\boldsymbol{q}' + \boldsymbol{e}) \wedge \boldsymbol{s} + \boldsymbol{A} &= \boldsymbol{0}, \\ \Omega' - \Delta + \beta &= 0, \end{aligned} \tag{16}$$

where $\boldsymbol{s} = \boldsymbol{R}^{\mathrm{T}}\boldsymbol{t}$, $\boldsymbol{S} = \boldsymbol{R}^{\mathrm{T}}\boldsymbol{T}\boldsymbol{R}$, $\boldsymbol{a} = \boldsymbol{R}^{\mathrm{T}}\boldsymbol{b}$, $\boldsymbol{A} = \boldsymbol{R}^{\mathrm{T}}\boldsymbol{B}\boldsymbol{R}$, whose components in the fixed basis are

$$\begin{aligned} \boldsymbol{s} &= N\boldsymbol{D}_1 + Q\boldsymbol{D}_2, \\ \boldsymbol{S} &= M\boldsymbol{D}_2 \wedge \boldsymbol{D}_1, \\ \boldsymbol{a} &= a_1\boldsymbol{D}_1 + a_2\boldsymbol{D}_2, \\ \boldsymbol{A} &= A\boldsymbol{D}_2 \wedge \boldsymbol{D}_1 \end{aligned} \tag{17}$$

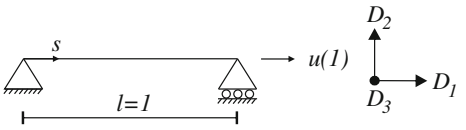

Fig. 1 Axial end displacement

2.3 Beam Subjected to an Axial End Displacement

In the following we will consider the case of the strut shown in Fig. 1 and look for solutions in which $\vartheta \equiv v \equiv 0$ so that expressions (10) reduce to

$$\begin{aligned} \varepsilon &= u', \\ \delta, \quad \delta' \end{aligned} \tag{18}$$

In addition, we will assume that the continuum is hyperelastic and its strain energy density written as

$$\pi(\varepsilon, \delta, \delta'), \tag{19}$$

which means that the only stress measures different from zero will be

$$N(\varepsilon, \delta, \delta') = \frac{\partial \pi}{\partial \varepsilon}, \quad \Delta(\varepsilon, \delta, \delta') = \frac{\partial \pi}{\partial \delta}, \quad \Omega(\varepsilon, \delta, \delta') = \frac{\partial \pi}{\partial \delta'}, \tag{20}$$

while $Q \equiv M \equiv 0$ and the definitions (17) if the body actions vanish, becomes

$$\begin{aligned} N' &= 0, \\ \Omega' - \Delta &= 0 \end{aligned} \tag{21}$$

By assuming the boundary conditions

$$\begin{aligned} \Omega(0) = \Omega(1) = 0, \\ u(0) = 0, \quad u(1) = \text{assigned} \end{aligned} \tag{22}$$

the Eqs. (18), (20), (21) and (22) constitute a nonlinear boundary value problem (see Aminpour et al. 2014; Aminpour and Rizzi 2015; Antman 2005) that will be discussed in the following.

3 Graphene

Graphite is a layered 3D material which is made up of a successive series of parallel two-dimensional sheets, called graphene sheets. A graphene sheet is a single layer of graphite which has only one atom in the thickness. Each graphene sheet is

composed of a regular hexagonal network of strongly bonded carbon atoms. Within each graphene sheet the distance between two adjacent carbon atoms is (Saito et al. 1998)

$$a_{\mathrm{c-c}} = 0.142 \times 10^{-9}\ \mathrm{m} = 1.42\ \text{Å}, \tag{23}$$

while its thickness is assumed to be

$$t = 3.4\ \text{Å} \tag{24}$$

A two-dimensional graphene sheet can be described as a lattice of regular hexagons, whose vertices show the position of the atoms and the edges describe the bonds (see Fig. 2). In the same figure, the parallelogram drawn in shadow is the unit cell (or REV) of the sheet and the vectors $\boldsymbol{a}_1$ and $\boldsymbol{a}_2$ are the basis vectors of the unit cell. The whole lattice can be generated by translations of the unit cell by the vectors

$$\boldsymbol{C}_{\mathrm{h}} = n\boldsymbol{a}_1 + m\boldsymbol{a}_2, \tag{25}$$

where n, m are integers. The vector $\boldsymbol{C}_{\mathrm{h}}$ is called the chiral vector of the sheet.

Two atoms whose positions (say $\boldsymbol{B}_1$ and $\boldsymbol{B}_2$) can be expressed by means of a chiral vector—which means that there are two integers n, m such that

$$\boldsymbol{B}_2 - \boldsymbol{B}_1 = \boldsymbol{C}_{\mathrm{h}}$$

are called equivalent. It is clear that the two atoms in the unit cell are not equivalent as

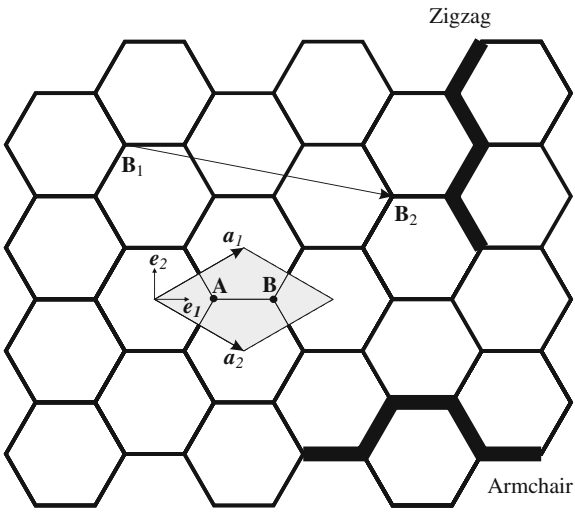

Fig. 2 Graphene sheet and its unit cell (or REV)

$$\boldsymbol{B} - \boldsymbol{A} = \frac{\boldsymbol{a}_1 + \boldsymbol{a}_2}{3} \tag{26}$$

In view of the following applications, it is useful to introduce an orthonormal basis $(\boldsymbol{e}_1, \boldsymbol{e}_2)$ whose two vectors are directed along the so called armchair and zigzag directions, respectively (see Fig. 2). Through the new basis, the basis vectors of the cell can be written as

$$\begin{aligned} \boldsymbol{a}_1 &= a\left(\frac{\sqrt{3}}{2}\boldsymbol{e}_1 + \frac{1}{2}\boldsymbol{e}_2\right), \\ \boldsymbol{a}_2 &= a\left(\frac{\sqrt{3}}{2}\boldsymbol{e}_1 - \frac{1}{2}\boldsymbol{e}_2\right), \end{aligned} \tag{27}$$

which give

$$\begin{aligned} \boldsymbol{a}_1 \cdot \boldsymbol{a}_1 &= \boldsymbol{a}_2 \cdot \boldsymbol{a}_2 = a^2, \\ \boldsymbol{a}_1 \cdot \boldsymbol{a}_2 &= a^2/2, \end{aligned} \tag{28}$$

where a is the lattice constant which is related to the carbon-carbon bond length $a_{\mathrm{c-c}}$ by the relationship

$$a = \sqrt{3} a_{\mathrm{c-c}} = 0.246 \times 10^{-9}\ \mathrm{m} \tag{29}$$

4 Energy

The total potential energy of the nanostructure may be given by the sum of energies due to the interatomic interactions (Rappe et al. 1992)

$$U = U_r + U_\theta + U_\tau + U_\omega + U_{\mathrm{vdW}} + U_{\mathrm{es}}, \tag{30}$$

where U_r is the bond stretching energy, U_θ is the bond angle bending energy, U_τ is the bond torsion (or dihedral angle variation) energy, U_ω is the bond inversion (or out of plane angle variation) energy, U_{vdW} is van der Waals interaction energy, and U_{es} is the electrostatic interaction energy.

Following Leamy (2007) for the terms $U_r + U_\theta$ in Eq. (30) we will assume the Modified Morse interatomic potential, that is

$$\begin{aligned} U_r &= D_e\left\{\left(1 - \mathrm{e}^{-\beta_e(r-r_0)}\right)^2 - 1\right\}, \\ U_\theta &= \frac{1}{2}k_\theta\,(\theta - \theta_0)^2\left\{1 + k_{\mathrm{sextic}}(\theta - \theta_0)^4\right\}, \end{aligned} \tag{31}$$

in which D_e, β_e, k_θ, k_{sextic} are constitutive constants, r is the length of a bond and θ is the angle between two adjacent bonds in the present configuration, while r_0 and θ_0 are the corresponding values in the reference configuration. The terms U_τ, U_ω,

U_{vdW} and U_{es}, on the contrary, will be neglected according to Xiao et al. (2005). This means that the expression (30) reduces to

$$U = U_r + U_\theta \tag{32}$$

5 Atomic Model

Figure 3 shows the reference configuration of the unit cells directed along the armchair and zigzag directions, respectively. The REV has been enlarged in order to consider the first neighbours of the two atoms in it. Let us assume that the sheet is stretched in the direction of the y axis in each one of the cases in Fig. 3 that are referred to as armchair and zigzag, respectively.

The displacement of an atom which occupies the reference position E, is described by the vector (see Fig. 4)

$$\boldsymbol{d}_E = v_E \boldsymbol{e}_1 + u_E \boldsymbol{e}_2 \tag{33}$$

The reference configuration of the enlarged REV is obtained by specifying the coordinates of each one of the six points in which are located the atoms. By assuming a local Cartesian coordinate system with origin at the middle point of the segment AB and basis $(\boldsymbol{e}_1, \boldsymbol{e}_2)$, the coordinates of a point E, will be denoted $E \equiv (x_E, y_E)$.

The reference configuration of the REV can also be completely specified when we fix the position of an atom and give the five bond lengths and the six angles between adjacent bonds. Note that the six angles are not independent because the sum of the three angles formed by the bonds that meet at the positions A and B, must be 2π. In the deformed configuration the new position occupied by the atom that in the reference configuration was in E, will be denoted by $e \equiv (x_e, y_e)$, where

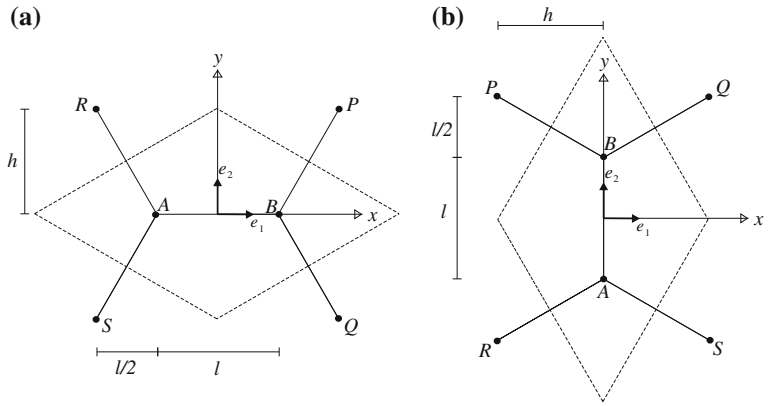

Fig. 3 The armchair (a) and zigzag (b) REVs

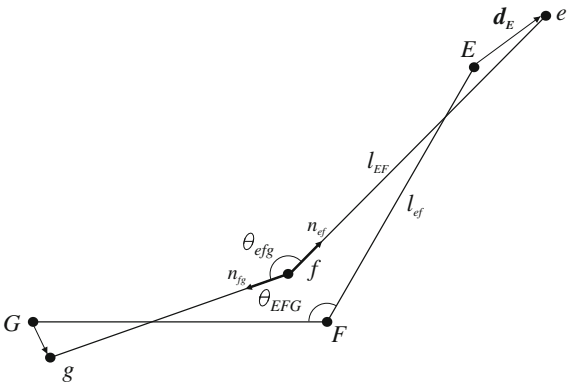

Fig. 4 Reference and present configuration of two adjacent bonds

$$\begin{aligned} x_e &= x_E + v_E, \\ y_e &= y_E + u_E \end{aligned} \tag{34}$$

In this way, the new length of a bond, say EF, results to be

$$\begin{aligned} \ell_{ef} &= |f - e| = \sqrt{(x_f - x_e)^2 + (y_f - y_e)^2} \\ &= \sqrt{[(x_F - x_E) + (v_F - v_E)]^2 + [(y_F - y_E) + (u_F - u_E)]^2}, \end{aligned} \tag{35}$$

while the angle between two adjacent bonds, say ef and fg is obtained from the relationship (see Fig. 4)

$$\cos \vartheta_{efg} = \boldsymbol{n}_{ef} \cdot \boldsymbol{n}_{fg}, \tag{36}$$

where

$$\begin{aligned} \boldsymbol{n}_{ef} &= \frac{e - f}{\ell_{ef}}, \\ \boldsymbol{n}_{fg} &= \frac{g - f}{\ell_{fg}} \end{aligned} \tag{37}$$

are the unit vectors along the bonds ef, and fg in the present configuration, respectively.

In view of the Eqs. (35)–(37), we define as deformation measures, the bonds' stretching and the angles' variation

$$\begin{aligned} \Delta r_{EF} &= \ell_{ef} - \ell_{EF}, \\ \Delta \vartheta_{EFG} &= \vartheta_{efg} - \vartheta_{EFG} \end{aligned} \tag{38}$$

Now, if we put

$$\begin{aligned} \Delta v_{EF} &= v_F - v_E, \\ \Delta u_{EF} &= u_F - u_E \end{aligned} \tag{39}$$

we can write

$$\begin{aligned} \ell_{ef} &= \sqrt{[(x_F - x_E) + \Delta v_{EF}]^2 + [(y_F - y_E) + \Delta u_{EF}]^2}, \\ \cos\vartheta_{efg} &= \frac{1}{\ell_{ef}\ell_{fg}}[(x_F - x_E + \Delta v_{EF})(x_G - x_F + \Delta v_{GF}) \\ &\quad + (y_F - y_E + \Delta u_{EF})(y_G - y_F + \Delta u_{GF})] \end{aligned} \tag{40}$$

and expressions (38) can be rewritten in terms of the components of the relative displacements.

6 1D Continuum Equivalent to the Atomic Model

The kinematic of the REV described in Sect. 5 and that of the continuum described in Sect. 2, are related by postulating the following relationships

$$\begin{aligned} u_E &= y_E \varepsilon(s), \\ v_E &= [\delta(s) + y_E \delta'(s)] x_E, \end{aligned} \tag{41}$$

where E stands for the position of a generic atom in the reference configuration of the REV and the abscissa of the 1D continuum has been chosen to coincide with the y axis on the REV, that is $s = y$.

Using the relationships (41), the components of the relative displacements of two atoms which form a C-C bond and in the reference configuration are in the positions E, F, will be

$$\begin{aligned} \Delta u_{EF} &= (y_F - y_E)\,\varepsilon, \\ \Delta v_{EF} &= (x_F - x_E)\delta + (x_F y_F - x_E y_E)\delta' \end{aligned} \tag{42}$$

Now, in view of the relationships (42), (40) and (38), the energy (31) is given in terms of the deformation measures of the continuum model

$$\begin{aligned} U_{EF}(\varepsilon, \delta, \delta') &= D_e \left\{ \left(1 - \mathrm{e}^{-\beta_e(\ell_{ef} - \ell_{EF})}\right)^2 - 1 \right\}, \\ U_{EFG}(\varepsilon, \delta, \delta') &= \frac{1}{2} k_\vartheta \left(\vartheta_{efg} - \vartheta_{EFG}\right)^2 \left\{1 + k_{\text{sextic}}(\,\vartheta_{efg} - \vartheta_{EFG})^4\right\} \end{aligned} \tag{43}$$

Summing up the contribution of all the bonds of the enlarged REV, one obtains

$$\begin{aligned}\hat{\pi}(\varepsilon,\delta,\delta') = U_{AB} + \frac{1}{2}U_{BP} + \frac{1}{2}U_{BQ} + \frac{1}{2}U_{AR} + \frac{1}{2}U_{AS} \\ + U_{RAB} + U_{ABP} + U_{SAB} + U_{ABQ} + U_{PBQ} + U_{RAS}\end{aligned} \tag{44}$$

By giving a power expansion up to the third order of $\hat{\pi}(\varepsilon,\delta,\delta')$ with respect to its arguments, we denote by $\check{\pi}(\varepsilon,\delta,\delta')$ the approximation obtained.

If we denote by V the volume of the REV, the strain energy density of the 1D continuum *equivalent* to the nanomaterial is assumed to be

$$\pi(\varepsilon,\delta,\delta') = \frac{1}{V}\check{\pi}(\varepsilon,\delta,\delta') \tag{45}$$

Making the derivatives of the strain energy density with respect to the components of the deformation measures, one obtains the components of the stress measures.

They result to have the following expressions for both the armchair and zigzag cases

$$\begin{aligned} N &= \frac{1}{V}\left(A\delta + \frac{1}{2}B\delta^2 + \frac{1}{2}C\delta'^2 + F\varepsilon + E\varepsilon\delta + \frac{1}{2}G\varepsilon^2\right), \\ \Delta &= \frac{1}{V}\left(P\delta + \frac{1}{2}R\delta^2 + \frac{1}{2}S\delta'^2 + A\varepsilon + B\varepsilon\delta + \frac{1}{2}E\varepsilon^2\right), \\ \Omega &= \frac{1}{V}(H\delta' + S\delta\delta' + C\varepsilon\delta') \end{aligned} \tag{46}$$

The explicit expressions for the constitutive coefficients have been evaluated for the following four cases using the MATHEMATICA software (Wolfram 2015)

- case a_1 armchair REV considering the sole stretching energy;
- case a_2 armchair REV considering stretching and angle variation energy;
- case b_1 zigzag REV considering the sole stretching energy;
- case b_2 zigzag REV considering stretching and angle variation energy.

As the resulting expressions are very cumbersome, in the following we give only the constitutive functions for the case a_1, that are

$$\begin{aligned} N = \frac{\partial\pi}{\partial\varepsilon} = \frac{1}{V}\Bigg[& 2\frac{h^4\beta_e^2 D_e\varepsilon}{\ell^2} + \frac{1}{2}h^2\beta_e^2 D_e\delta \\ & + \left(\frac{3}{4}\frac{h^4\beta_e^2 D_e}{\ell^2} - 3\frac{h^6\beta_e^3 D_e}{\ell^3}\right)\varepsilon^2 \\ & + \left(-\frac{1}{8}h^2\beta_e^2 D_e + \frac{1}{4}\frac{h^4\beta_e^2 D_e}{\ell^2} - \frac{3}{16}h^2\beta_e^3 D_e\ell\right)\delta^2 \\ & + \left(\frac{1}{8}h^2\beta_e^2 D_e - \frac{h^4\beta_e^2 D_e}{\ell^2} - \frac{3}{2}\frac{h^4\beta_e^3 D_e}{\ell}\right)\varepsilon\delta \end{aligned} \tag{47}$$

$$+\left(-\frac{1}{2}h^2\beta_{\mathrm{e}}^2 D_e+\frac{h^4\beta_{\mathrm{e}}^2 D_e}{\ell^2}-\frac{3}{4}h^2\beta_{\mathrm{e}}^3 D_e\ell\right)\delta'^2\Bigg],$$

$$\begin{aligned}\Delta=\frac{\partial\pi}{\partial\delta}=\frac{1}{V}\Bigg[&\frac{1}{2}h^2\beta_{\mathrm{e}}^2 D_e\varepsilon\\&+\left(\frac{1}{8}\beta_{\mathrm{e}}^2 D_e\ell^2+\frac{1}{4}\beta_{\mathrm{e}}^2 D_e\ell^2+h^2\beta_{\mathrm{e}}^2 D_e\right)\delta\\&+\left(\frac{1}{16}h^2\beta_{\mathrm{e}}^2 D_e-\frac{1}{2}\frac{h^4\beta_{\mathrm{e}}^2 D_e}{\ell^2}-\frac{3}{4}\frac{h^4\beta_{\mathrm{e}}^3 D_e}{\ell}\right)\varepsilon^2\\&+\left(\frac{3}{16}h^2\beta_{\mathrm{e}}^2 D_e-\frac{3}{64}\beta_{\mathrm{e}}^3 D_e\ell^3-\frac{3}{2}\beta_{\mathrm{e}}^3 D_e\ell^3\right)\delta^2\\&-\left(\frac{1}{4}h^2\beta_{\mathrm{e}}^2 D_e\ell^4+\frac{1}{2}\frac{h^4\beta_{\mathrm{e}}^2 D_e}{\ell^2}-\frac{3}{8}h^2\beta_{\mathrm{e}}^3 D_e\ell\right)\varepsilon\delta\\&+\left(\frac{3}{4}h^2\beta_{\mathrm{e}}^2 D_e-\frac{3}{16}\beta_{\mathrm{e}}^3 D_e\ell^3\right)\delta'^2\Bigg],\end{aligned}\tag{48}$$

$$\begin{aligned}\Omega=\frac{\partial\pi}{\partial\delta'}=\frac{1}{V}\Bigg[&\frac{1}{2}\beta_{\mathrm{e}}^2 D_e\delta'+\left(\frac{3}{2}h^2\beta_{\mathrm{e}}^2 D_e-\frac{3}{8}\beta_{\mathrm{e}}^3 D_e\ell^3\right)\delta\delta'\\&-\left(h^2\beta_{\mathrm{e}}^2 D_e+2\frac{h^4\beta_{\mathrm{e}}^2 D_e}{\ell^2}-\frac{3}{2}h^2\beta_{\mathrm{e}}^3 D_e\ell\right)\varepsilon\delta'\Bigg],\end{aligned}\tag{49}$$

where h and ℓ are shown in Fig. 3.

7 Beam with End Displacement: Trivial Solution

Let us consider now the case of a beam described in Sect. 2.3 and let $u_\ell = u(\ell)$ be the axial displacement assigned to the end section. The boundary value problem (18), (21), (22), (46), admits the following trivial solution

$$\begin{aligned}&\Omega_o\equiv 0,\quad \Delta_o\equiv 0,\quad \delta_o'\equiv 0,\quad \varepsilon_o'\equiv 0,\\&\varepsilon_o = u_\ell/\ell = u_\ell\quad(\text{as } \ell=1),\\&\delta_o = \delta(u_\ell),\\&N_o = N(\varepsilon(u_\ell),\delta(u_\ell))\end{aligned}\tag{50}$$

By using the chain rule it can be seen that

$$\begin{aligned}\frac{\mathrm{d}N_o}{\mathrm{d}u_\ell}&=\frac{\mathrm{d}N_o}{\mathrm{d}\varepsilon_o}=(\frac{\partial N}{\partial\varepsilon})_o+(\frac{\partial N}{\partial\delta})_o(\frac{\partial\delta}{\partial\varepsilon})_o,\\\frac{\mathrm{d}\Delta_o}{\mathrm{d}u_\ell}&=\frac{\mathrm{d}\Delta_o}{\mathrm{d}\varepsilon_o}=(\frac{\partial\Delta}{\partial\varepsilon})_o+(\frac{\partial\Delta}{\partial\delta})_o(\frac{\partial\delta}{\partial\varepsilon})_o,\end{aligned}\tag{51}$$

where $(\,)_o$ means that the expression is evaluated along the solution (50).

As on the trivial path,

$$\Delta_o = 0 \quad \Rightarrow \quad \frac{\mathrm{d}\Delta_o}{\mathrm{d}\varepsilon_o} = 0 \tag{52}$$

Equation $(51)_2$ gives

$$(\frac{\partial \delta}{\partial \varepsilon})_o = -\frac{(\frac{\partial \Delta}{\partial \varepsilon})_o}{(\frac{\partial \Delta}{\partial \delta})_o} \tag{53}$$

and by substituting (53) in the equation $(51)_1$ one obtains

$$\frac{\mathrm{d}N_o}{\mathrm{d}\varepsilon_o} = \frac{(\frac{\partial N}{\partial \varepsilon})_o(\frac{\partial \Delta}{\partial \delta})_o - (\frac{\partial N}{\partial \delta})_o(\frac{\partial \Delta}{\partial \varepsilon})_o}{(\frac{\partial \Delta}{\partial \delta})_o} \tag{54}$$

8 Perturbation Method

We are interested in looking for another solution branching off from the given (fundamental) one. Besides, we assume that the branching solution can be expressed in terms of a suitable parameter η, in the form

$$\Xi^b(s, \eta) = \Xi_o(s, p(\eta)) + \Xi(s, \eta) \tag{55}$$

where Ξ stands for a generic field and p is the parameter chosen to describe the trivial solution that, in general, is different from η.

We admit that the functions can be represented by the following power expansions near the bifurcation point that corresponds to $\eta = 0$

$$\begin{aligned} \Xi^b(s, \eta) &= \Xi_c(s) + \Xi_1^b(s)\,\eta + \frac{1}{2}\Xi_2^b(s)\,\eta^2 + o(\eta^2), \\ \Xi_o(s, \eta) &= \Xi_c(s) + \Xi_{o1}(s)\,\eta + \frac{1}{2}\Xi_{o2}(s)\,\eta^2 + o(\eta^2), \end{aligned} \tag{56}$$

$$p(\eta) = p_c + p_1\,\eta + \frac{1}{2}p_2\,\eta^2 + o(\eta^2), \tag{57}$$

in which the subscript c denotes the value of a function at the bifurcation point ($\eta = 0$) while the other subscripts denote differentiation with respect to η evaluated at $\eta = 0$, as well.

Using the expansion (56) for both $\Xi^b(s,\eta)$, and $\Xi_o(s,p(\eta))$, Eq. (55) gives

$$\Xi(s,\eta) = \Xi_1(s)\,\eta + \frac{1}{2}\Xi_2(s)\,\eta^2 + o(\eta^2) \tag{58}$$

The aim of the analysis is to obtain the coefficients of the series expansion in terms of η, of the sliding variables $\varepsilon, \delta, N, \Delta, \Omega$ and of the parameter p, up to a given order. To do that we use a perturbation technique so that, making use of the expansions (56) and (58), the *nonlinear* BVP stated in Sect. 2.2 is transformed in a sequence of *linear* BVPs, one for each power of η.

9 Beam with End Displacement: Bifurcation Analysis

The first order (linear) counterpart of the nonlinear BVP results to be

$$\varepsilon_1 = u_1', \tag{59}$$

$$\begin{aligned} N_1' &= 0,\\ \Omega_1' - \Delta_1 &= 0, \end{aligned} \tag{60}$$

$$\begin{aligned} N_1 &= A\delta_1 + B\delta_c\delta_1 + F\varepsilon_1 + E\delta_c\varepsilon_1 + E\varepsilon_c\delta_1 + G\varepsilon_c\varepsilon_1,\\ \Delta_1 &= P\delta_1 + R\delta_c\delta_1 + A\varepsilon_1 + B\delta_c\varepsilon_1 + B\varepsilon_c\delta_1 + E\varepsilon_c\varepsilon_1,\\ \Omega_1 &= H\delta_1' + S\delta_c\delta_1' + C\varepsilon_c\delta_1', \end{aligned} \tag{61}$$

$$\begin{aligned} \Omega_1(0) &= \Omega_1(1) = 0,\\ u_1(0) &= u_1(1) = 0 \end{aligned} \tag{62}$$

Now by substituting (62) into Eq. (60) one obtains

$$\begin{aligned} A\delta_1' + B\delta_c\delta_1' + F\varepsilon_1' + E\delta_c\varepsilon_1' + E\varepsilon_c\delta_1' + G\varepsilon_c\varepsilon_1' &= 0,\\ H\delta_1'' + S\delta_c\delta_1'' + C\varepsilon_c\delta_1'' - (P\delta_1 + R\delta_c\delta_1 + A\varepsilon_1 + B\delta_c\varepsilon_1 + B\varepsilon_c\delta_1 + E\varepsilon_c\varepsilon_1) &= 0 \end{aligned} \tag{63}$$

Equation $(63)_1$, then gives

$$\varepsilon_1' = -\frac{A + B\delta_c + E\varepsilon_c}{F + E\delta_c + G\varepsilon_c}\,\delta_1' \tag{64}$$

and, by taking the first derivative of Eq. $(63)_2$ with respect to s, making use of Eqs. $(62)_3$ and (64), one obtains

$$\Omega_1'' + q(u_\ell)\Omega_1 = 0, \tag{65}$$

where

$$q(u_\ell) = -\frac{(F + E\delta_c + G\varepsilon_c)(P + R\delta_c + B\varepsilon_c) - (A + B\delta_c + E\varepsilon_c)^2}{(H + S\delta_c + C\varepsilon_c)(F + E\delta_c + G\varepsilon_c)}, \tag{66}$$

which results to be

$$q(u_\ell) = -\frac{(\frac{\partial N}{\partial \varepsilon})_o(\frac{\partial \Delta}{\partial \delta})_o - (\frac{\partial N}{\partial \delta})_o(\frac{\partial \Delta}{\partial \varepsilon})_o}{(\frac{\partial N}{\partial \varepsilon})_o(\frac{\partial \Omega}{\partial \delta'})_o} \tag{67}$$

Note that Eq. (65) is the one reported by Antman (2005). It admits a non trivial solution for any positive integer n such that

$$-\frac{(\frac{\partial N}{\partial \varepsilon})_o(\frac{\partial \Delta}{\partial \delta})_o - (\frac{\partial N}{\partial \delta})_o(\frac{\partial \Delta}{\partial \varepsilon})_o}{(\frac{\partial N}{\partial \varepsilon})_o(\frac{\partial \Omega}{\partial \delta'})_o} = n^2\pi^2 \tag{68}$$

Equation (68) determines the values $u_{\ell c}$ corresponding to the bifurcation points. The eigenmode associated to the first eigenvalue, is

$$\Omega_1 = C_1 \sin \pi s \tag{69}$$

Then we can integrate the expressions $(62)_3$ to obtain

$$\delta_1 = -\frac{C_1}{\pi}\frac{\cos \pi s}{H + S\delta_c + C\varepsilon_c} + C_2 \tag{70}$$

In addition, from Eq. $(60)_2$

$$\Delta_1 = \Omega_1' = C_1 \pi \cos \pi s \tag{71}$$

and, from the expression $(62)_2$

$$\varepsilon_1 = \frac{C_1 \pi \cos \pi s}{A + B\delta_c + E\varepsilon_c} + \frac{P + R\delta_c + B\varepsilon_c}{A + B\delta_c + E\varepsilon_c}\left(\frac{C_1 \cos \pi s}{\pi(H + S\delta_c + C\varepsilon_c)} - C_2\right) \tag{72}$$

and Eq. (59) gives then the displacement in the form

$$u_1 = \frac{C_1 \sin \pi s}{A + B\delta_c + E\varepsilon_c} + \frac{P + R\delta_c + B\varepsilon_c}{A + B\delta_c + E\varepsilon_c}\left(\frac{C_1 \sin \pi s}{\pi^2(H + S\delta_c + C\varepsilon_c)} - C_2 s\right) + C_3 \tag{73}$$

Finally, the boundary condition $(62)_3$ gives

$$C_3 = 0 \tag{74}$$

and, the boundary condition $(62)_4$ gives C_2. The constant C_1 is the amplitude of the eigenmode and can be assigned a value by choosing a normalization condition.

10 Beam with End Displacement: Numerical Results

We consider the REV in Fig. 3a and assume that the atoms, in the reference configuration, have the following coordinates

$$\begin{array}{llll} x_A = -\ell/2 & y_A = 0 & x_B = \ell/2 & y_B = 0 \\ x_R = -\ell & y_R = h & x_P = \ell & y_P = h \\ x_S = -\ell & y_S = -h & x_Q = \ell & y_Q = -h \end{array} \tag{75}$$

Similarly, the coordinates of the atoms in the REV in Fig. 3b are

$$\begin{array}{llll} x_A = 0 & y_A = -\ell/2 & x_B = 0 & y_B = \ell/2 \\ x_R = -h & y_R = -\ell & x_P = -h & y_P = \ell \\ x_S = h & y_S = -\ell & x_Q = h & y_Q = \ell \end{array} \tag{76}$$

Following Belytschko et al. (2002) the geometric and constitutive constants in the energy expressions (43) are given the following values

$$\begin{array}{lll} \ell = 0.142 \text{ nm} & h = 0.123 \text{ nm} & \theta_0 = 2.094 \text{ rad} \\ D_e = 0.603105 \text{ nN}\times\text{nm} & k_\theta = 0.9 \text{ nN}\times\text{nm} \times \text{rad}^{-2} & \\ \beta_e = 26.25 \text{ nm}^{-1} & k_{\text{sextic}} = 0.754 \text{ rad}^{-4} & \end{array} \tag{77}$$

From the coordinates (76) its is evident that the REV has width $w = 3\ell$ and height $2h$. Denoting by t its thickness, the volume appearing in (49) is $V = 3\ell h t$ and, for $t = 0.34$ nm, $V = 0.0178\,\text{nm}^3$. Using the preceding data the numerical values for the constitutive coefficients in (62) have been evaluated for the four cases considered and are given in Table 1. In addition, the normal force as a function of u_ℓ in the trivial solution has been determined and is plotted in Fig. 5 only for the cases a_2 and b_2.

Table 1 Constitutive coefficients

	A	B	C	E	F	P	G	R	S	H
case a1	6.28	−15.99	−0.96	−60.58	18.86	18.85	−144.1	−188.54	−0.06	0.12
case a2	4.26	−17	−0.94	−55.52	20.88	20.87	−153.2	−191.58	−0.17	0.16
case b1	6.04	−32.65	−0.65	−0.81	19.41	17.16	−181.92	−111.92	−2.25	0.34
case b2	4.88	−29.71	−0.59	−1.7	20.69	18.42	−183.74	−116.28	−2.34	0.37

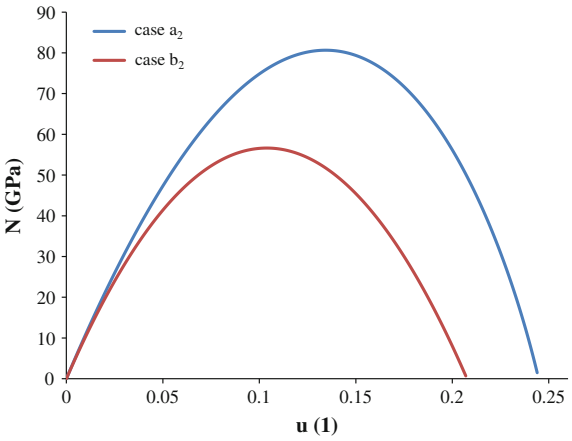

Fig. 5 Trivial path

Table 2 Values of the apparent Young's modulus

	Young's modulus (TPa)
case a1, case b1	0.94
case a2, case b2	1.12

Finally the values of the *apparent* Young's modulus—which is defined as the slope at the origin of the trivial path—that is

$$E = \left(\frac{\partial N_o}{\partial \varepsilon}\right)_{\varepsilon=0},$$

have been calculated. The values obtained for all the four cases are reported in Table 2. In Table 3 the results obtained by some other authors are reported for the sake of comparison. It can be seen that they are very close to those given in Table 2.

The bifurcation points along the trivial path can be obtained from Eq. (68) and the smaller values for u_ℓ are obtained by putting $n = 1$. In Fig. 6 the curve $q(u_\ell) - \pi^2$ for the case a_2, is plotted. Bifurcation occurs when the curve crosses the u_ℓ axis, that is when $u_\ell = 0.136$. Now, as the maximum value of the normal force is reached for $u_\ell = 0.133$ (see Fig. 5) the bifurcation occurs just a little bit after the limit point.

Table 3 Comparison of Young's modulus

Reference	Modeling method	Young's modulus (TPa)
Lee et al. (2008)	Experimental	1 ± 0.1
van Lier et al. (2000)	Density functional theory	1.11
WenXing et al. (2004)	Molecular dynamic	1.02
Xiao et al. (2005)	Nano scale- Continuum	1.13
Wu et al. (2006)	Nano scale- Continuum	1.06

We want to stress that the asymptotes in Fig. 6 correspond to the values of u_ℓ at which

$$(\frac{\partial N}{\partial \varepsilon})_o$$

and

$$\left(\frac{\partial \Omega}{\partial \delta'}\right)_o$$

do vanish, respectively. This means that the constitutive functions obtained for the equivalent beam are not strongly elliptic and this is due, in turn, to the fact that the Modified Morse potential is not convex. In Fig. 7 the curve $q(u_\ell) - \pi^2$ for the case b_2, is plotted. In this case bifurcation occurs when $u_\ell = 0.106$.

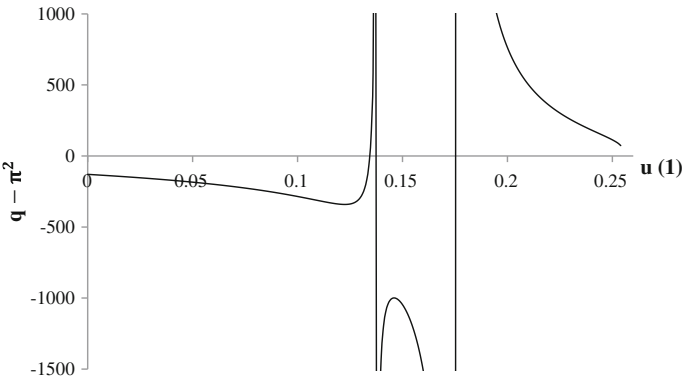

Fig. 6 Armchair arrangement: bifurcation plot

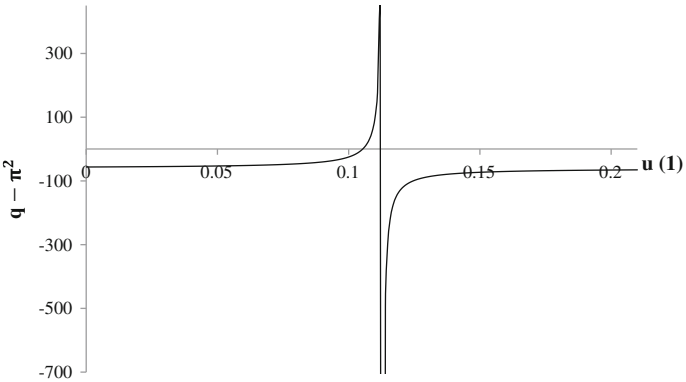

Fig. 7 Zigzag arrangement: bifurcation plot

The maximum value of the normal force, instead, is reached for $u_\ell = 0.101$ (see Fig. 5) so that, as before, bifurcation occurs after the limit point. In this case only one asymptote is present. It is located at the value of u_ℓ at which

$$(\frac{\partial N}{\partial \varepsilon})_o = 0$$

We want to stress that, looking at the values of the end displacement reported before, one can conclude that in both examined cases the bifurcation point practically coincides with the limit point of the curve $N(u_\ell)$. Looking at the shape of the component δ_1 of the buckling mode, given by the expressions (74), it is clear that such a solution describes a necking phenomenon.

11 Conclusions

A procedure that leads to the identification of constitutive functions for a hyperelastic 1D continuum endowed with a suitable internal structure able to describe the mechanics behaviour of carbon nano structures, has been introduced. A graphene sheet with armchair and zigzag structures have been considered and a representative elementary volume identified. An equilibrium configuration is assumed as a reference configuration for the REV. When the atoms are displaced in a generic configuration, the variation of the energy of the REV is evaluated by using the Modified Morse interatomic potential. A displacement field of the 1D model is put in relation with displacement of the atoms in the REV. By using this map, the energy variation of the REV is written on terms of the deformation measures of the 1D model. This expression, divided by the volume of the REV is assumed as the strain energy density of the continuum. The stress measures and their constitutive functions are then obtained by differentiating the strain energy density with respect to the 1D deformation measures. As an example, the Young's modulus of a carbon nano sheet has been evaluated and compared with the values reported it the literature. The two cases of a sheet stretched in the armchair or zigzag direction, respectively, have been studied and a bifurcation which describes a necking phenomenon, detected.

References

Alibert J, Seppecher P, dell'Isola F, (2003) Truss modular beams with deformation energy depending on higher displacement gradients. Math Mech Solids 8(1):51–73

Altenbach H, Bîrsan M, Eremeyev V (2012) On a thermodynamic theory of rods with two temperature fields. Acta Mech 223(8):1583–1596

Aminpour H, Rizzi N (2015) A 1D continuum with microstructure for single-wall CNTs bifurcation analysis. Math Mech Solids 114. doi:10.1177/1081286515577037

Aminpour H, Rizzi N, Salerno G (2014) A one-dimensional beam model for single-wall carbon nano tube column buckling. In: Topping B, Ivnyi P (eds) Proceedings of the twelfth international conference on computational structures technology. Civil-Comp Press, Stirlingshire

Antman S (2005) Nonlinear problems of elasticity, applied mathematical sciences, vol 107. Springer, New York

Belytschko T, Xiao S, Schatz G, Ruoff R (2002) Atomistic simulations of nanotube fracture. Phys Rev B 65(23):235–430

Bîrsan M, Altenbach H, Sadowski T, Eremeyev V, Pietras D (2012) Deformation analysis of functionally graded beams by the direct approach. Compos Part B: Eng 43(3):1315–1328

di Carlo A (1996) A non-standard format for continuum mechanics. In: Batra R, Beatty M (eds) Contemporary research in the mechanics and mathematics of materials. CIMNE, Barcelona

dell'Isola F, Seppecher P, Madeo A, (2012) How contact interactions may depend on the shape of Cauchy cuts in Nth gradient continua: approach 'à la D'Alembert'. ZAMP 63(6):1119–1141

Germain P (1973a) La méthode des puissance virtuelles en mécanique des milieux continus, 1ère partie: la théorie du second gradient. J de Mécanique 12(2):235–274

Germain P (1973b) The method of virtual power in continuum mechanics, II: microstructure. SIAM J Appl Math 25(3):555–575

Leamy MJ (2007) Bulk dynamic response modeling of carbon nanotubes using an intrinsic finite element formulation incorporating interatomic potentials. Int J Solids Struct 44(3–4):874–894

Lee C, Wei X, Kysar J, Hone J (2008) Measurement of the elastic properties and intrinsic strength of monolayer graphene. Science 321(5887):385–388

van Lier G, van Alsenoy C, van Doren V, Geerlings V (2000) Ab initio study of the elastic properties of single-walled carbon nanotubes and graphene. Chem Phys Lett 326(1–2):181–185

Pei Q, Zhang Y, Shenoy V (2010) A molecular dynamics study of the mechanical properties of hydrogen functionalized graphene. Carbon 48(3):898–904

Pietraszkiewicz W, Eremeyev V, Konopińska V (2007) Extended non-linear relations of elastic shells undergoing phase transitions. ZAMM 87(2):150–159

Podio-Guidugli P (1982) Flexural instabilities of elastic rods. J Elast 12(1):3–17

Rappe AK, Casewit CJ, Colwell KS, Goddard WA III, Skiff WM (1992) UFF, a rule-based full periodic table force field for molecular mechanics and molecular dynamics simulations. J Am Chem Soc 114(25):10,024–10,035

Saito R, Dresselhaus G, Dresselhaus MS (1998) Physical properties of carbon nanotubes. Imperial College Press, London

Shima H, Sato M (2013) Elastic and plastic deformation of carbon nanotubes. CRC Press, Boca Raton

WenXing B, ChangChun Z, WanZhao C (2004) Simulation of Young's modulus of single-walled carbon nanotubes by molecular dynamics. Physica B 352(1–4):156–163

Wolfram (2015) Mathematica, Version 10.3. Imperial College Press, Champaign

Wu Y, Zhang X, Leung A, Zhang W (2006) An energy-equivalent model on studying the mechanical properties of single-walled carbon nanotubes. Thin-Walled Struct 44(6):667–676

Xiao JR, Gamaa BA, Gillespie JW Jr, (2005) An analytical molecular structural mechanics model for the mechanical properties of carbon nanotubes. Int J Solids Struct 42(11–12):3075–3092

http://www.springer.com/978-3-319-31719-9

Generalized Continua as Models for Classical and Advanced Materials

Altenbach, H.; Forest, S. (Eds.)
2016, XII, 457 p. 104 illus., 48 illus. in color., Hardcover
ISBN: 978-3-319-31719-9